cAMP controls rod photoreceptor sensitivity via multiple targets in the phototransduction cascade

Luba A. Astakhova, Evgeniia V. Samoiliuk, Victor I. Govardovskii, and Michael L. Firsov

I.M. Sechenov Institute of Evolutionary Physiology and Biochemistry, Russian Academy of Sciences, 194223 St. Petersburg, Russia

In early studies, both cyclic AMP (cAMP) and cGMP were considered as potential secondary messengers regulating the conductivity of the vertebrate photoreceptor plasma membrane. Later discovery of the cGMP specificity of cyclic nucleotide–gated channels has shifted attention to cGMP as the only secondary messenger in the phototransduction cascade, and cAMP is not considered in modern schemes of phototransduction. Here, we report evidence that cAMP may also be involved in regulation of the phototransduction cascade. Using a suction pipette technique, we recorded light responses of isolated solitary rods from the frog retina in normal solution and in the medium containing 2 µM of adenylate cyclase activator forskolin. Under forskolin action, flash sensitivity rose more than twofold because of a retarded photoresponse turn-off. The same concentration of forskolin lead to a 2.5-fold increase in the rod outer segment cAMP, which is close to earlier reported natural day/night cAMP variations. Detailed analysis of cAMP action on the phototransduction cascade suggests that several targets are affected by cAMP increase: (a) basal dark phosphodiesterase (PDE) activity decreases; (b) at the same intensity of light background, steady background-induced PDE activity increases; (c) at light backgrounds, guanylate cyclase activity at a given fraction of open channels is reduced; and (d) the magnitude of the Ca^{2+} exchanger current rises 1.6-fold, which would correspond to a 1.6-fold elevation of $[Ca^{2+}]_{in}$. Analysis by a complete model of rod phototransduction suggests that an increase of $[Ca^{2+}]_{in}$ might also explain effects (b) and (c). The mechanism(s) by which cAMP could regulate $[Ca^{2+}]_{in}$ and PDE basal activity is unclear. We suggest that these regulations may have adaptive significance and improve the performance of the visual system when it switches between day and night light conditions.

INTRODUCTION

Vertebrate rod and cone photoreceptors convert absorbed light stimuli into graded electrical responses at their output synapse by means of the G protein–coupled receptor–based phototransduction cascade. In this cascade, the light-sensitive receptor, rhodopsin, activates the cGMP-specific type 6 phosphodiesterase (PDE) via the G protein transducin, as recently reviewed (Burns and Baylor, 2001; Lamb and Pugh, 2006; Yau and Hardie, 2009; Arshavsky and Burns, 2012). In the early studies of molecular mechanisms of phototransduction, both cAMP (Bitensky et al., 1971) and cGMP (Miki et al., 1973; Lipton et al., 1977) were considered as potential secondary messengers regulating the conductivity of the photoreceptor plasma membrane. A later discovery of the cGMP specificity of CNG channels in the photoreceptor plasma membrane (Fesenko et al., 1985) has shifted attention to cGMP as the sole second messenger in the vertebrate phototransduction cascade, and cAMP is not usually considered either a messenger or a modulator in the modern schemes of phototransduction.

However, there is accumulating evidence that cAMP may also control photoreceptor signaling. Recent studies of retinal circadian rhythms reveal significant changes in the cAMP content in the whole mouse retina (Nir et al., 2002) and in cultured chicken photoreceptors (Chaurasia et al., 2006). These changes are controlled by two pathways. One pathway involves dopamine (Nir et al., 2002) and calcium (Ivanova et al., 2008), and the other involves dopamine-dependent acceleration of the synthesis of type 1 adenylate cyclase (Jackson et al., 2009). Variations in the cAMP level control the rate of melatonin synthesis in photoreceptors (Iuvone and Besharse, 1986; Pierce et al., 1989), which in turn affects dopamine release from the inner retina, thus creating a feedback loop that drives the day/night cycle of retinal functions (Tosini et al., 2008). Furthermore, cAMP affects photoreceptor photomechanical movement in fish (Burnside et al., 1982) and amphibians (Besharse et al., 1982) and synaptic Ca^{2+} current in salamander photoreceptors (Stella and Thoreson, 2000).

cAMP has multiple potential targets within the phototransduction cascade itself. Several key proteins of the cascade have been reported as substrates of PKA: bovine guanylate cyclase (GC) (Wolbring and Schnetkamp, 1996) and GC-activating protein (Peshenko et al., 2004);

---

human (Horner et al., 2005), *Xenopus laevis* (Osawa et al., 2008), and mice (Osawa et al., 2011) rhodopsin kinases GRK7 and GRK1; and phosducin (Pagh-Roehl et al., 1995; Willardson et al., 1996). cAMP-dependent phosphorylation modifies the affinity of cone CNG channel to cGMP (Ko et al., 2004). Moreover, GRK7 and GRK1 are phosphorylated in a light-dependent manner (Osawa et al., 2008, 2011).

Large-scale changes of the cAMP content in photoreceptor cells during the day/night cycle and the existence of targets for cAMP-dependent phosphorylation in the phototransduction cascade suggest that the cascade may be regulated by cAMP. However, this regulation has not yet been shown in intact photoreceptor cells, and an attempt to detect cAMP regulation in dialyzed outer segments of gecko rods was unsuccessful (Jindrova and Detwiler, 2000). Here, we present evidence that a pharmacologically induced increase of the cAMP content in isolated rods of *Rana ridibunda* frog evokes distinct changes in the phototransduction cascade. Perfusion with cell-permeating cAMP analogues or application of the nonspecific activator of adenylate cyclase, forskolin, led to a significant increase in the photoreceptor sensitivity. Detailed physiological analysis of cAMP action on the phototransduction cascade suggests that several proteins are affected. cAMP elevated cytoplasmic Ca^{2+} by possibly increasing the fraction of the rod outer segment (ROS) current carried by Ca^{2+}. Another effect was a 1.6-fold decrease of the basal PDE activity in the dark. Finally, high cAMP level extended the lifetime of the transducin-activated PDE by slowing its turn-off processes. We suggest that naturally occurring changes in the cAMP content of rod photoreceptors during the day/night cycle may up- and down-regulate the phototransduction cascade, thereby adjusting its efficiency to specific lighting conditions.

MATERIALS AND METHODS

Photocurrent recordings
R. ridibunda adult frogs were caught in the wild in southern Russia, kept for up to 6 mo with free access to water at 10–15°C on a natural day/night cycle, and fed living cockroaches and dry pet food. Frogs were treated in accordance with the Guide for the Care and Use of Laboratory Animals (1996. National Academy of Sciences, Washington, DC) and with the rules approved by the local Institutional Animal Care and Use Committee. Before the experiment, animals were dark-adapted overnight. Eyes were enucleated and the retina was extracted under dim red light. Then a small piece of retina was transferred under infrared surveillance into a small Petri dish, shred by two forceps, and pipetted several times to obtain isolated rods with preserved inner segments. Suction recording was performed basically as devised by Baylor et al. (1979). The specific details of our suction setup design and functioning have been described (Astakhova et al., 2008). In the majority of experiments, rods were recorded in an "outer segment out" configuration. In attempts to localize the site of drug action, we also recorded from rods that were sucked outer segment in, thus exposing the inner segment to the perfusion solution. Fast solution change

around the exposed rod compartment was achieved with a two-barrel local perfusion system operating under stepper motor control. It allowed replacing a basic physiological solution with either of two test solutions of different composition within ~50 ms. Cells were stimulated with 10-ms flashes and/or steady backgrounds of LED light at λ_{max} = 525 nm (two independent channels). Responses were recorded with 100-Hz digitization, except records of 3-isobutyl-1-methylxanthine (IBMX)-induced responses where digitization was 500 Hz, and low-pass filtered at 30 Hz (eight-pole Bessel filter). Flash intensity was calibrated for most of individual rods using the statistics of few-photon responses (Baylor et al., 1979) and confirmed by measurements with a calibrated photometer.

Main Ringer's solution referred to as normal contained (in mM): 90 NaCl, 2.5 KCl, 1.4 $MgCl_2$, 1.05 $CaCl_2$, 5 $NaHCO_3$, 5 HEPES, and 0.05 EDTA, pH adjusted to 7.6. Forskolin- and IBMX-containing solutions were normal solution plus 2 µM forskolin (Sigma-Aldrich) or 0.2 mM IBMX, respectively, added from fresh stock solutions in DMSO. Final concentration of DMSO in the perfusion solution was 0.02% (forskolin) or 0.033% (IBMX). Corresponding concentrations of pure DMSO in normal solution had no statistically significant effects on the rod dark current and photoresponse. The temperature was held at 17–19°C.

Correction of photoresponse to photocurrent compression
Generally, changes in sensitivity can be determined from amplitudes of flash responses, r, if the responses are well within the linear range, that is, $r << r_{max}$, where r_{max} is the maximum response amplitude at saturating flashes. Real responses do not usually obey this restriction and are compressed because of saturation. Therefore, to estimate real effects of forskolin on sensitivity, we corrected response amplitude values for saturation by calculating imaginary "linear" responses (normalized to r_{max}) as $r_{lin} = r/(1 - r)$, assuming Michaelis-like saturation (Astakhova et al., 2008).

Measurement of steady PDE activity in darkness and in constant light: Limitation of the dark current by inner segment
The cGMP turnover rate β was determined by quickly applying to the cell a high concentration of the PDE inhibitor IBMX, as suggested by Hodgkin et al. (1985) and Hodgkin and Nunn (1988), and described in detail by Astakhova et al. (2008). The application of IBMX led to a fast increase of the circulating current, and β value before the jump could be determined as the slope of $(j_{post}/j_{pre})^{1/3}$ versus time function. However, in many dark-adapted cells, the increase of the current was quite modest, and a low signal-to-noise ratio precluded accurate determination of β. We tentatively attribute this behavior to the fact that isolated rods, especially in the frog, usually lack the synaptic terminal and a part of the cell body. Then the resistance of the inner segment is likely increased compared with an intact cell, and maximum ROS current in these cells could be limited by the inner segment. On the other hand, light adaptation decreases the ROS conductance so the limitation by the inner segment becomes less severe. Therefore, the responses to IBMX application in light-adapted rods posed no problem for the analysis.

Stability of the records
A full protocol to measure PDE activity at different background lights in normal and forskolin-containing solution included ~20 applications of IBMX solution and usually lasted ~50 min. Therefore, the metabolic stability of the recorded cell during the prolonged experiment had to be ascertained. As a control, we periodically measured the dark current of the cell by applying saturating flashes. Only the cells without significant degradation of the dark current during the record were chosen for further analysis. The averaged ratio of the dark current at the end of the protocol to its initial value in normal Ringer's solution was

0.93 ± 0.03 (n = 17; P < 0.03). In control experiments, the same illumination levels and jumps to IBMX were applied to rods in normal Ringer's solution. The dark current exhibited small (<5%) irregular variations of either sign; no statistically significant decline was observed during the entire protocol. However, the sensitivity of weak flash responses at the end of the protocol could decrease by ≤25%, and their kinetics could accelerate. We attribute this behavior to the light adaptation caused by accumulated rhodopsin bleaching, which could reach 0.1%. Because the action of forskolin on the flash response was opposite to the effect of light adaptation (see Results), we conclude that possible changes of the cell's metabolic and adaptation state could only lead to a slight underestimate of the effect of forskolin.

cAMP measurement

Before cAMP measurements, all frogs were kept on 12-d/12-night cycle for at least 1 wk. Animals were used between 3- and 5-h Zeitgeber time. After eye enucleation and vitreous removal, the eyeball was cut into two to four segments and the retina was detached and placed on filter paper, outer segments up. The specimens were then put into small Petri dishes containing normal or forskolin Ringer's solution. For "forskolin" protocol, a control retinal piece was kept in normal solution in darkness for the period of the longest forskolin exposure (1,000 s). Other pieces of the same retina were kept in forskolin-containing solution for 200, 600, and 1,000 s in darkness. For "light" protocol, all retinal pieces were kept in normal solution, with the control one in the dark and other ones illuminated by uniform light of saturating intensity for 1,000 s (LED source: λ_{max} = 525 nm, 1.85×10^4 photons · μm^{-2} s^{-1}). Then the pieces were removed from the solution and quickly pushed by the outer segments' side to a polished copper block cooled by liquid nitrogen (Govardovskii and Berman, 1981; Sokolov et al., 2002). After quick freezing, retinal pieces were placed on a cryotome-stage outer segments up, and the layer of outer segments was cut off at -22 °C. We used 10-μm-thick slices, and the position of the cryotome's cutting plane with respect to retinal layers could be checked by observing the purple color of the outer segments. Slices of outer segments were transferred to ice-cold 0.1 N HCl and immediately vortexed. Samples were sedimented at 2,000 g, supernatant was removed, and protein pellet was redissolved in 1 N NaOH. Protein content was measured by the Lowry method, and cAMP in supernatant was determined with a commercial EIA kit (Assay Designs) and normalized to protein content. To improve the accuracy of EIA measurement, each sample was divided into five separately measured aliquots.

Mathematical modeling

The mathematical model of phototransduction includes all firmly established biochemical mechanisms of phototransduction and its regulation by calcium feedback. A basic set of model equations is given earlier (Kuzmin et al., 2004; Kolesnikov et al., 2011). However, in contrast to Kolesnikov et al. (2011), the quenching of activated rhodopsin Rh* was supposed to proceed in two steps, namely Rh* phosphorylation and subsequent arrestin binding. Corresponding equations are given by Astakhova et al. (2008).

The parameters of the model were chosen to be within experimental biochemical and biophysical values when such data are available (Table S2). Some of these values (dark PDE activity β_{dark}, parameters of GC regulation by Ca^{2+}, time constant of arrestin binding τ_A) were either measured directly in our experiments or were inferred from our results. Still, there was a great flexibility of fitting, as various sets of other parameters allowed virtually perfect simulation of photoresponses. However, our goal was not to perfectly reproduce the responses but rather find out what parameters must be changed to simulate the effects of forskolin. Thus, once a good fit of a normal response was achieved, the fits of responses in forskolin solution were further constrained by

experimentally determined changes in β_{dark}, parameters of Ca^{2+} homeostasis, and GC regulation, with possible small adjustment of their values for each particular cell. The adjustments were within a standard deviation from experimentally determined averages. Then the only parameter left free for fitting was the rate constant of PDE* quenching, k_E. The fit was optimized by maximizing the coefficient of correlation between experimental and model traces, which was $r^2 \geq 0.995$.

Data analysis

Throughout this paper, data are presented as mean ± SEM. All experimental data were analyzed using STATISTICA software. In most cases, the effects of forskolin are expressed as a ratio of post- and pretreated parameters and analyzed with Student's t test for single means (α = 0.05).

Online supplemental material

The online supplemental material contains data on the concentration dependence of physiological effects of forskolin, and illustrates action of several inhibitors of cAMP-specific PDEs type 1–4 (vinpocetine, EHNA, cylostamide, rolipram, and Ro 20–174) and a permeable cAMP analogue, Sp-cAMPS, on photoresponse. It also includes a table of definitions and values of parameters used in the mathematical model of the photoresponse. The online supplemental material is available at http://www.jgp.org/cgi/content/full/jgp.201210811/DC1.

RESULTS

Dark level and light-induced changes of cAMP level

In normal Ringer's solution, dark level of cAMP in the photoreceptor outer segments was 7.3 ± 0.6 pmol/mg protein (n = 31 retina). Assuming that rhodopsin comprises 65% of ROS total proteins (summarized in Pugh and Lamb, 2000), rhodopsin concentration in ROS is 3.2 mM, and the cytoplasm volume is one half of the outer segment volume, the cAMP concentration in the ROS cytoplasm is equal to 2.9 μM. We also tested whether the cAMP level changes under minutes of light exposure. Retinas were incubated in normal Ringer's solution and
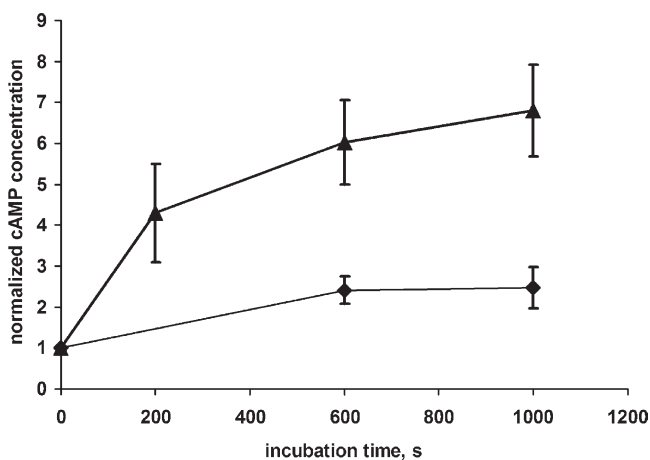
Figure 1. Effect of forskolin on cAMP content in frog retinal outer segment layer. Incubation with 2 μM (◆, six retinas) and 10 μM (▲, eight retinas) of forskolin (mean ± SEM). Concentrations are normalized to the value measured in normal Ringer's solution.
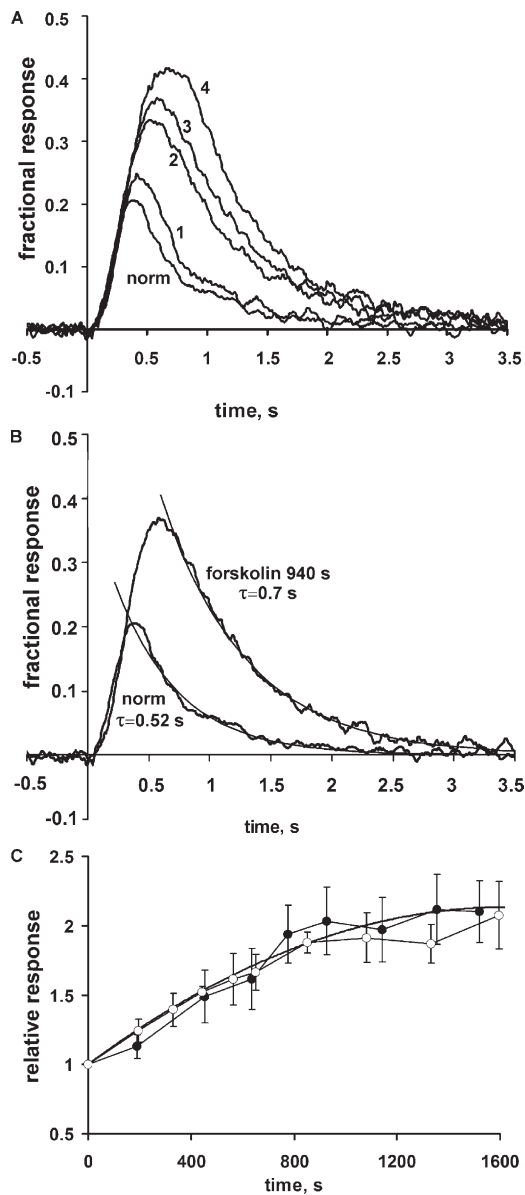
Figure 2. 2 μM forskolin increases photoreceptor sensitivity. (A) Responses at various time of incubation in forskolin-containing Ringer's solution. Response labeled "norm" was recorded in normal Ringer's solution just before the start of forskolin perfusion; 1–4 were recorded from the same cell after incubation with forskolin during 205, 610, 940, and 1,340 s, respectively. Flash intensity in all records was 0.82 photons · μm⁻² per flash. Responses are normalized to corresponding dark current that was 19 pA in normal solution and 18 pA at the end of perfusion with forskolin. Each trace is the average of eight responses. (B) A single-exponential fit of the falling phase of two photoresponses recorded in normal solution and in the presence of forskolin after 940 s of incubation. Same cell as in A. (C) Changes of rods' sensitivity during incubation in forskolin-containing Ringer's solution, in configuration inner segment in (○) and outer segment in (●). The site of the forskolin application has no effect either on the time course or the magnitude of the response. The sensitivity is measured by photoresponses to a weak flash. All individual responses are normalized first to corresponding dark current, and second to corresponding response in normal Ringer's solution. Initial normalized response amplitudes were ≈0.2. The same flash

exposed to saturating light of 1.85×10^4 photons · $\mu m^{-2} s^{-1}$ for 1,000 s before freezing. We found that light decreases cAMP concentration in the outer segment layer 1.26 ± 0.11 times ($n = 15$; P < 0.025).

Forskolin affects cAMP levels and increases light sensitivity in rod photoreceptors

To assess the effect of cAMP on photoreceptor function, we recorded electrical responses to light of solitary rods isolated from the frog retina. Rods were perfused either with a normal Ringer's solution or with the solution containing the activator of the adenylate cyclase forskolin. To evaluate the forskolin impact on cAMP, we first measured the cAMP level in the outer segment layer during incubation of the isolated retina in Ringer's solution containing 2 or 10 μM forskolin. We found that the cAMP level in the layer of ROS during 1,000 s of incubation increased 2.47 ± 0.46 (2 μM forskolin; $n = 6$; P < 0.02) or 6.80 ± 1.31 (10 μM forskolin; $n = 8$; P < 0.004) times from the original dark level of 7.3 pmol/mg protein (Fig. 1). Thus, the elevation of cAMP in ROS induced by 2 μM forskolin is close to the reported natural day/night variations of the cAMP level in photoreceptors (1.6–2.5-fold; Traverso et al., 2002; Ivanova and Iuvone, 2003; Fukuhara et al., 2004; Chaurasia et al., 2006; Li et al., 2008; see also Discussion) and can be considered as a physiological elevation. Therefore, we used 2 μM of forskolin-containing solution in further physiological experiments as a tool to imitate circadian variation of cAMP levels in photoreceptors.

In forskolin-containing solution, photoresponses to weak nonsaturating flashes increased because of a progressive delay of the photoresponse turn-off, whereas the rising phase of the photoresponse did not change noticeably (Fig. 2 A). The effect of forskolin was clearly concentration dependent. Its magnitude increased and it developed faster when the concentration of forskolin increased from 0.4 through 2 to 10 μM (Fig. S1). As explained above, we used a 2-μM concentration for further detailed analysis because it produced cAMP changes resembling those during circadian cycle. On average, the amplitude of photoresponses evoked by weak flashes in dark-adapted rods in 2 μM of forskolin solution increased by 2.12 ± 0.1–fold ($n = 17$; P < 0.0001). This rise of sensitivity developed rather slowly, with the maximum effect achieved between 15 and 25 min, and time of half-effect around 450 s (Fig. 2 C). During the initial period of perfusion, the growth of photoresponse

intensity was used throughout the entire time of incubation for each particular cell in a given recording configuration (an average of four cells in each configuration; mean ± SEM). The heavy smooth line is a parabolic approximation of pooled data for two configurations. It has no mechanistic meaning and is only used to characterize the time course of the effect of forskolin to be compared with the effects of other drugs.

amplitude in approximately half of rods was accompanied by a transient increase of the photoresponse delay by ~50 ms, which looked like a parallel shift of the entire rising phase to longer times. This effect disappeared after 7–10 min of perfusion. The cause of the effect is unclear.

The effect of applying 2 µM forskolin to the inner segment was indistinguishable from that produced via ROS (Fig. 2 C). The response sensitivity increase was accompanied by a concurrent slowdown of the photoresponse falling phase. In most cases, the falling phase could be fit with a single-exponential function whose time constant τ_{fall} monotonically increased with the incubation time in the forskolin-containing solution (Fig. 2 B). The average increase of the falling phase time constant at 15–20-min perfusion was $\frac{\tau_{fall}^{forsk}}{\tau_{fall}^{norm}}$ = 1.39 ± 0.09—fold ($n = 13$; P < 0.001).

The action of forskolin was not washable; i.e., moving a rod back to normal solution did not stop further slow development of both effects during at least 15 min of wash-out. The dark current was only slightly and irregularly affected by forskolin. The ratio of the dark current after 15 min of incubation in the forskolin-containing solution to the dark current before the forskolin application was 0.94 ± 0.03 ($n = 21$; P < 0.03), whereas a few cells exhibited a small (<10%) increase of the current.

The effect of forskolin was more prominent at high light backgrounds. The forskolin/normal Ringer's solution sensitivity ratio progressively increased with the decrease of the fraction of open channels. For example, in the dark-adapted state, the flash sensitivity was increased by 2.12-fold, whereas at backgrounds closing 60–80% of channels open in the dark, the sensitivity increased by 4.86 ± 0.91–fold ($n = 7$; P < 0.025).

In addition to forskolin, we have tested several other compounds that affect the intracellular level of cAMP. Among those were inhibitors of cAMP-specific PDEs 1, 2, 3, and 4: vinpocetine, EHNA, cilostamide, rolipram, Ro 20–174, and the cell-permeable cAMP analogue SP-cAMPS. All these compounds produced changes in photoresponse properties that closely resembled the changes evoked by forskolin (Fig. S2). Responses to nonsaturating flashes grew in size, kinetics of the photoresponse falling phase slowed down, and both effects were slowly developing (Table S1). In addition, the effect of rolipram and Ro 20–174 was partly reversible by wash-out (Fig. S2 D). These data suggest that the effect of forskolin was indeed mediated by cAMP elevation rather than a nonspecific action of forskolin on the phototransduction cascade.

High cAMP affects both dark and light-induced PDE activity

To analyze mechanisms of the photoreceptor sensitivity increase in the presence of forskolin, we monitored steady activity of PDE through various intensities of stationary light background in normal conditions and in the presence of forskolin. The PDE activity can be expressed as

$$\beta(t) = \beta_{dark} + \beta_l(t), \tag{1}$$

where β_{dark} is PDE activity in darkness, and $\beta_l(t)$ is activity evoked by light. In a steady state, $\beta_l(t) = \beta_s$, where β_s is the PDE activity evoked by the steady background light.

PDE activities at each specific intensity of background light or in darkness were measured by instant application of a nonspecific PDE inhibitor, IBMX (Hodgkin et al., 1985; Hodgkin and Nunn, 1988). The cell was driven for 0.5–1 s into a jet of Ringer's solution containing 0.2 mM IBMX, which evoked a large and fast rise of the outer segment current. Next, PDE activity β was obtained from analyzing the rising phase of the currents evoked by IBMX (for details see Materials and methods). A typical experimental sequence included the following steps. Flash responses of a rod cell were first recorded in normal Ringer's solution in the dark and under stationary light backgrounds of ascending intensities. After each change of the background light intensity, the cell was given time to stabilize the photocurrent. Then the resting photocurrent j_s was measured by applying a saturating flash. The flash was followed by a brief jump into the IBMX-containing solution to measure β. At some background light intensities, responses to nonsaturating flashes were repeatedly recorded. After turning the background light off, the cell was allowed to recover until it reached pre-background parameters of the photoresponse. The cell was next drawn into the forskolin-containing solution and held in darkness to let the effect develop, and then the procedure was repeated again.

In many cells, β_{dark} could not be reliably measured because of limitation of the circulating current by the conductivity of the inner segment in dark-adapted isolated rods (see Materials and methods). The same cells, however, exhibited a severalfold increase in the current when exposed to IBMX on a light-adapting background. To circumvent this problem, we measured β_{dark} on a subset of dark-adapted rods that produced a large magnitude (>50%) of IBMX-evoked response. In these cells, forskolin resulted in a marked decrease of β_{dark} (1.59 ± 0.12–fold; $n = 13$; P < 0.0004).

According to Eq. 1, the background-induced β_s is defined as the difference between β measured at a given background and β_{dark}. In the cells where β_{dark} was not measured directly, we used an average estimate of $\beta_{dark\ norm} = 0.49 ± 0.10$ s^{-1} ($n = 13$) for normal solution and $\beta_{dark\ forsk} = 0.49$ s^{-1}/1.59 = 0.31 s^{-1} for forskolin-containing solution. The values are about an order of magnitude smaller than typical β measured at 50% closed channels. Therefore, possible uncertainty of β_{dark} in each particular cell should not introduce a significant error into the resulting β_s estimate.

In accordance with the forskolin-induced increase of flash sensitivity, current responses to steady backgrounds also increased after forskolin perfusion (Fig. 3). The same was true for the background-induced β_s. Similarly to the flash sensitivity, this increase was more prominent at brighter backgrounds. Although at low background intensities $\beta_{s\ forsk}$ did not differ from $\beta_{s\ norm}$ within the experimental error, with increasing background light intensity, the ratio $\beta_{s\ forsk}/\beta_{s\ norm}$ increased approximately logarithmically (Fig. 4).

Forskolin apparently affects GC activity regulation by Ca²⁺
Once β at a given background is experimentally measured, the GC activity, α, can also be calculated as follows. cGMP concentration normalized to its dark value is
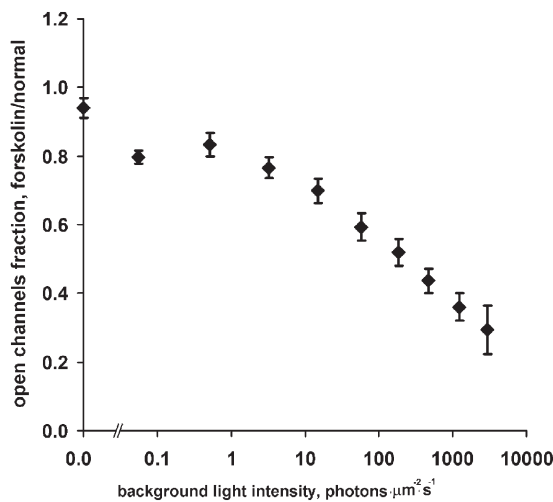
$$\frac{cG}{cG_{dark}} = \left(\frac{j_s}{j_{dark}}\right)^{1/n_{cG}}, \qquad (2)$$

where j_s is the resting photocurrent at a particular light background intensity, j_{dark} is the dark photocurrent of the same rod, and $n_{cG} = 3$ is the Hill's coefficient of the channels' regulation by cGMP. On the other hand, in a steady state,

$$cG = \frac{\alpha}{\beta}. \qquad (3)$$

Hence,

$$\alpha = cG_{dark} \cdot \beta \cdot \left(\frac{j_s}{j_{dark}}\right)^{1/3}. \qquad (4)$$

Figure 3. Forskolin reduces the fraction of open channels at all intensities of the background light. The ordinate axis represents the ratio of fractions of open channels in the forskolin-containing and normal solutions. The value at the zero background intensity corresponds to the dark-adapted cell measurements.

Regulation of the GC activity by Ca²⁺ could be described by a Hill-type equation:

$$\alpha(Ca) = \alpha_{min} + (\alpha_{max} - \alpha_{min}) \cdot \left(1 - \frac{Ca^{n_{cyc}}}{Ca^{n_{cyc}} + K_{cyc}^{n_{cyc}}}\right). \qquad (5)$$

Here, α_{max} is the maximum GC activity at zero Ca, α_{min} is the minimum activity at high Ca, K_{cyc} equals Ca at half-effect, and n_{cyc} is the Hill coefficient reflecting the cooperative character of the cyclase regulation (Koch and Stryer, 1988). Fitting the α_s versus j_s/j_{dark} curve with the Hill equation shows a consistent shift of the forskolin curve toward a smaller percentage of open channels (Fig. 5). Here, the fraction of the open channels at half-effect (which is supposed to be proportional to K_{cyc}) decreases considerably ($K_{cyc\ forsk}/K_{cyc\ norm} = 0.73 \pm 0.05$; $n = 18$; P < 0.0001). Maximum GC activity also decreases
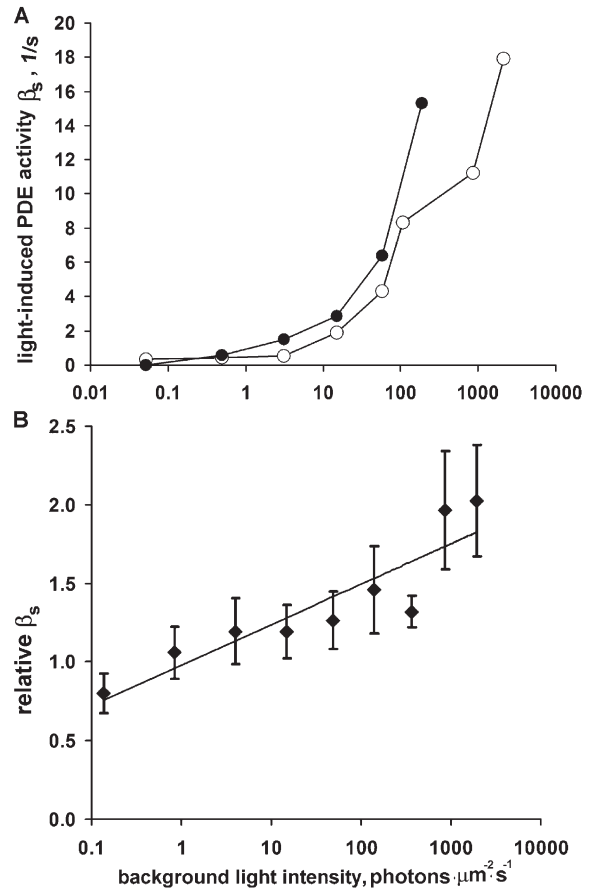
Figure 4. Forskolin affects light-induced steady PDE activity, β_s. (A) β_s of a single rod in normal (○) and forskolin-containing (●) solutions versus light background intensity in log scale. (B) Averaged ratio $\beta_{s\ forsk}/\beta_{s\ norm}$ versus light background intensity in log scale (14 cells). Error bars represent SEM. The straight line is drawn by a least-square procedure with parameters y = 0.11*ln(x) + 1.56. It has no mechanistic meaning and is only used to show general trend of the data.
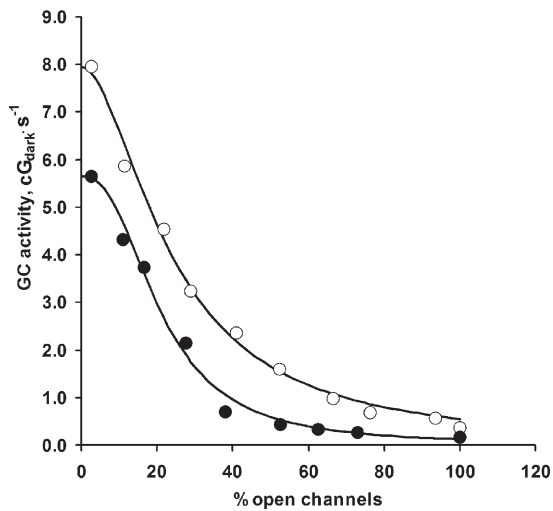
Figure 5. Forskolin modifies Ca^{2+} regulation of GC. GC activity in normal (○) and forskolin-containing (●) solution versus fraction of open channels. Here, "100% open channels" refers to the situation in dark. The same cell as in Fig. 4 A. The lines are drawn using the Hill equation with K_{cyc} = 24% and n = 1.8 in normal solution and K_{cyc} = 20.9% and n = 2.5 in forskolin-containing solution.

$(\alpha_{max\ forsk}/\alpha_{max\ norm} = 0.71 \pm 0.07;\ n = 15)$, whereas the change of the Hill coefficient n is statistically insignificant $(n_{forsk}/n_{norm} = 0.90 \pm 0.07;\ n = 18;\ P < 0.15)$.

Forskolin affects Ca^{2+} homeostasis in ROS

Shift of the α_s versus j_s/j_{dark} curve by forskolin may indicate a modification of the GC modulation by Ca^{2+}. The kinetics of at least one of the turn-off reactions, R^* phosphorylation by rhodopsin kinase, is also known to

be controlled via a Ca^{2+} feedback loop (Arshavsky and Burns, 2012). Therefore, we tested whether forskolin affects the Ca^{2+} homeostasis in ROS. Kinetics of light-induced calcium changes was characterized by measuring the exchanger current. In a steady state, the Ca^{2+} influx through the CNG channels in ROS is counterbalanced by its extrusion by the electrogenic $Na^+/Ca^{2+}–K^+$ exchanger located in the ROS plasma membrane (Nakatani and Yau, 1989; Lagnado et al., 1992). When CNG channels are instantaneously closed by a bright saturating stimulus, the exchanger keeps working for some time, reducing the cytoplasmic Ca^{2+} concentration to a new steady-state level. This is seen as a slow, approximately exponential creeping of the photoresponse to a steady (zero) current level that follows a fast rising phase caused by the closure of the CNG channels (Fig. 6). Because of the stoichiometry of the exchanger $((1\ Ca^{2+} + 1\ K^+): 4Na^+)$, the initial magnitude of the exchanger current is half of the preceding inward Ca^{2+} current through the channels and approximately proportional to $[Ca^{2+}]_{in}$. Its time integral is one half of the charge of the extruded cytoplasmic Ca^{2+}.

The magnitude of the exchanger current is routinely estimated from an exponential approximation of the top of a saturated response. However, the position of starting point for fitting is dubious, mostly because of the uncertainty of the moment when all CNG channels are closed. Combined with the recording noise, this makes the estimation of parameters of the exchanger current by curve fitting rather inaccurate. We found that the parts of saturated responses that supposedly reflect the exchanger current in normal Ringer's solution and in forskolin solution can be made congruent by a
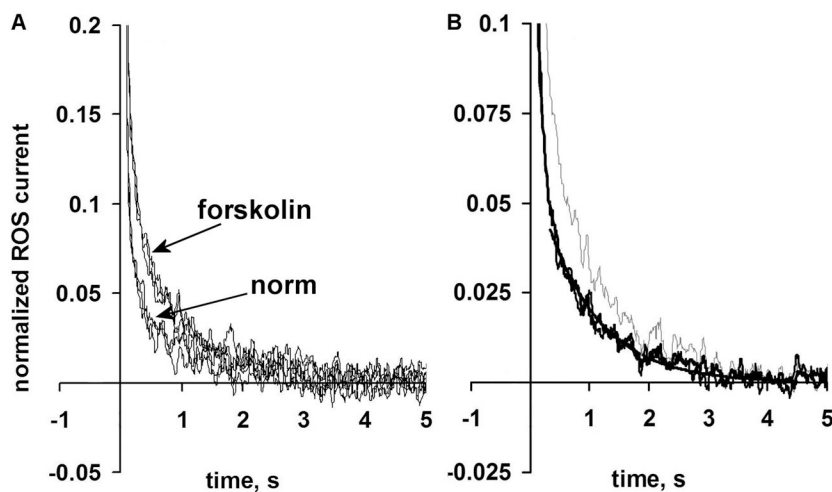
Figure 6. Forskolin enhances the Ca^{2+} exchanger current. (A) Light-insensitive tail of the ROS current in responses to bright saturating flashes is well-reproducible. Three traces in each group are individual responses to three 10-ms flashes of ascending intensities that resulted in a >10-s saturation time (2,270, 3,880, and 6,610 photons $\cdot$ µm^{-2}). Dark current was 20.7 pA in normal Ringer's solution and 21.9 pA in forskolin solution. Recordings labeled *forsk* were done between 16 and 18 min after the start of forskolin perfusion. (B) Exchanger currents in forskolin solution and normal Ringer's solution can be made congruent by amplitude scaling. Thin noisy lines are averages of corresponding three traces in A. Bold noisy line shows the current in forskolin solution downscaled by 1.68-fold to match the current recorded in normal Ringer's solution. The scaling factor was found by maximizing the cross-correlation coefficient between the two curves. The heavy smooth line is a single-exponential approximation of averaged normal and downscaled forskolin responses. Fraction of the exchanger current, 0.062; decay time constant, 0.91 s.

mere amplitude scaling. That is, if the transform $i_{scaled}(t) = i_{unscaled}/k$ is applied to the normalized response in forskolin, the resulting $i_{scaled}(t)$ curve, after proper adjustment of the scaling factor $k > 1$, coincides with the corresponding part of the photoresponse in normal solution (Fig. 6 B; notice that here we use the flowing current i rather than the photocurrent r for clarity). In 12 of 13 cells processed this way, the match between the two curves was quite good, yielding the coefficient of correlation >0.99 for low-noise responses. In one cell, time courses of the exchanger currents in normal Ringer's solution and forskolin solution were significantly different, so reasonable scaling was not possible. This cell was excluded from the analysis.

We found that forskolin increases the magnitude of the exchanger current by 1.64 ± 0.033–fold ($n = 12$) without significantly changing its decay time constant. Obviously, the current integral also increased by the same factor, pointing to the corresponding increase of the exchangeable Ca^{2+} fraction in ROS. An average decay time constant determined by a single-exponential fitting was 0.78 ± 0.05 s, and the fraction of the exchanger current in normal Ringer's solution was 0.069 ± 0.004. This translates into a 0.138 fraction of the dark current carried by Ca^{2+}, in a good agreement with earlier estimates (summarized in Pugh and Lamb, 2000).

Forskolin increases dominant recovery time constant

As revealed by the Pepperberg plot (Pepperberg et al., 1992), perfusion with forskolin retarded rod's recovery from supersaturating flashes. The increase of the dominant recovery time constant, τ_D, was moderate but
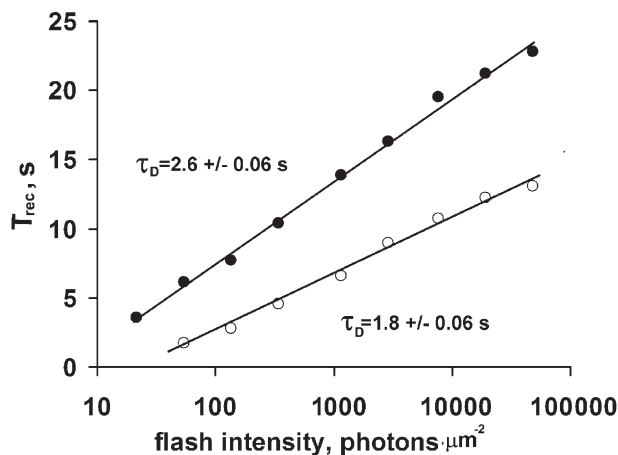
Figure 7. Forskolin increases the dominant time constant of the PDE shut-off. Plot of the time of recovery from saturation (T_{rec}) as a function of the flash intensity in the log scale in normal (○) and forskolin-containing (●) solution. T_{rec} is defined as the time of regaining 20% of dark current. Straight lines are an approximation of experimental points with $T_{rec} = c + \tau_D*ln(I)$. Numbers at the lines show corresponding dominant recovery time constants, τ_D. The cell with the biggest effect of forskolin is shown. Records in forskolin solution were started after 15 min of perfusion.

statistically significant, on average 1.17 ± 0.04–fold (13 cells). Fig. 7 shows the plots for the cell with the largest effect. Previously we have shown that τ_D in *R. ridibunda* characterizes neither rhodopsin nor transducin quenching but probably represents the time constant of arrestin binding to phosphorylated $R*$ (Astakhova et al., 2008).

DISCUSSION

Effect of forskolin and light on ROS cAMP content

We have found that exposures of frog rods to factors increasing their intracellular cAMP level, such as perfusion with forskolin or cell-permeable cAMP analogues, resulted in marked changes of the photoresponse. Although multiple biochemical evidence suggests that cAMP and its effector PKA may regulate components of the phototransduction cascade, experimental testing of the cAMP impact on the phototransduction was only made in a single study (Jindrova and Detwiler, 2000) in which neither cAMP nor 8-bromo-cAMP affected photoresponses of internally dialyzed outer segments of gecko rods. The absence of any effect in this study could be caused by the loss of some critical components required for the cAMP-dependent regulation of phototransduction or altered calcium homeostasis in dialyzed ROS. However, the lack of the cAMP effects in the experiments of Jindrova and Detwiler (2000) may also indicate that the targets for cAMP action are localized in the inner segment. This possibility will be discussed below.

We have found that the dark level of cAMP in the frog ROS in normal Ringer's solution was 7.3 pmol/mg protein. This is close to the cAMP levels in other retinas (in pmol/mg protein): 8.5 (*Xenopus*; Hasegawa and Cahill, 1999), ∼17 (zebrafish embryos; Li et al., 2008), and ∼10 (suspension of cultured chicken photoreceptors; Ivanova and Iuvone, 2003; Chaurasia et al., 2006) at day Zeitgeber time. Perfusion with 2 µM forskolin led to a 2.5-fold increase of the cAMP content in the ROS layer. This increase is within the same range as 1.6- to 2.5-fold oscillations of the total content of cAMP in whole retina preparations during day/night cycle (rats: Traverso et al., 2002; Fukuhara et al., 2004; zebrafish embryos: Li et al., 2008; culture of chicken photoreceptor cells: Ivanova and Iuvone, 2003; Chaurasia et al., 2006). Hence, we suppose that the forskolin-induced 2.5-fold increase of cAMP in the frog outer segment layer is a close imitation of the cAMP changes during a diurnal cycle.

In contrast to diurnal oscillations, the problem of short-term light-induced changes of cAMP content in photoreceptors is less clear. In *Xenopus*, strong light exposure of the retina during 10–25 min does not produce measurable changes of the cAMP content (Hasegawa and Cahill, 1999). On the other hand, in rat

(Nir et al., 2002) and mouse (Jackson et al., 2009), cAMP level reduces twofold after 7–10 min of bright background light in the presence of 1 mM IBMX. We found a moderate 1.26-fold decrease of the cAMP level in ROS within 15 min of saturating light exposure. It appears that light-induced cAMP changes in minute ranges are markedly smaller than diurnal changes.

Physiological effects of elevated cAMP level

The application of 2 µM forskolin for 15 min caused a 2.1-fold increase in the photoreceptor sensitivity to brief flashes of light by slowing down the response turn-off, whereas the amplification in the cascade remained unchanged (Fig. 2 A). It also increased the fraction of the CNG channels closed at a given steady background light (Fig. 3). The effects are reminiscent of the effect of the Na^+-K^+-ATPase inhibitor strophanthidin (Demontis et al., 1995). Thus, the question arises of whether the observed changes result from a specific action of cAMP on the phototransduction cascade, or they simply reflect a metabolic rundown of the cell. Obviously, metabolic rundown should primarily suppress the dark current, as indeed observed by Demontis et al. (1995). Contrary to this, the dark current remained remarkably stable in our experiments (See Materials and methods). Besides, we have seen no effect of forskolin on the kinetics of the exchanger current (Fig. 6 B), whereas deterioration of the cell is expected to decrease the exchanger activity by reducing its driving force. Thus, we suggest that the metabolic state of the rod was not significantly affected by our treatments, and that the effects of elevated cAMP level are caused by its specific action on intracellular targets. Reversibility of the effects of rolipram and Ro-20-174 also argues against the cell deterioration.

Possible mechanisms of cAMP action

The observed effects could be produced either by a cAMP-induced modification of the cascade turn-off or by a modification of the Ca^{2+} feedback, or both. To distinguish between the two possibilities, we have measured steady activities of PDE in darkness and at various light backgrounds with and without forskolin. These measurements were used to calculate the GC activity as a function of the fractional resting current.

The analysis rests on the assumption that the measurements with IBMX jumps provide an accurate estimate of the pre-jump PDE activity. Specifically, the question arises as to whether the inhibition of the PDE by IBMX is instantaneous and complete. As for the speed of IBMX action, it seems high enough because the calculated PDE activity evoked by bright backgrounds increases >20-fold compared with the dark value, without a clear sign of saturation (Fig. 4 A). There is no guarantee, however, that the inhibition of PDE by 0.2 mM IBMX is complete. Incomplete inhibition would lead to an underestimated PDE activity and the GC

activity derived from it. This error is probably not big because bright backgrounds led to >20-fold GC activation with respect to its dark-adapted state (Fig. 5). This is close to maximum activation expected from in vitro data on Ca^{2+} dependency of the GC activity (Peshenko et al., 2011). Therefore, we believe that the data on PDE and GC activities derived from IBMX-jump experiments are not seriously compromised by possible insufficient speed and completeness of IBMX action.

Our analysis revealed that both PDE and Ca^{2+} feedback are likely to be affected. For PDE, the effect consisted of a decrease of its basal dark activity β_{dark} and an increase in the steady light-induced activity β_s. For GC, the entire activity versus (j_s/j_{dark}) curve shifted toward lower j_s/j_{dark} levels.

A possible mechanism(s) of β_{dark} control by cAMP is unclear. The γ subunit of PDE, Pγ, is reportedly phosphorylated at a PKA-specific site, threonine 35 (Thr35) (Xu et al., 1998; Paglia et al., 2002; Janisch et al., 2009), and it was found in vitro that phosphorylation of Pγ at either Thr22 or Thr35 causes a minor decrease in its ability to inhibit PDE (Paglia et al., 2002). This suggests that in vivo phosphorylation should increase the dark PDE activity, reduce the dark current, and accelerate the photoresponse. Instead, we find the opposite: high cAMP level (hence phosphorylation of proteins) decreases β_{dark} and slows down the photoresponse without affecting the dark current. Also, replacing Thr35 with alanine (hence abolishing Pγ phosphorylation) decreases the sensitivity of photoresponse and reduces dark current in mice rods (Tsang et al., 2007), again opposite of the prediction from the in vitro results. Thus, available biochemical data provide no clue for explaining the effect of cAMP on β_{dark}.

The background-induced steady PDE activity β_s increases because of a retardation of the turn-off processes. In principle, the retardation of the cascade turn-off(s) and shift of the GC activity versus (j_s/j_{dark}) curve toward lower j_s/j_{dark} levels could be caused by a sole factor, namely, elevated dark concentration of the cytoplasmic Ca^{2+}. Indeed, such elevation can be inferred from the exchanger current measurements. As shown in Fig. 6, forskolin resulted in an ~1.6-fold increase of the magnitude of the exchanger current. If properties of the exchanger are not affected by cAMP, this increase would correspond to a similar elevation of $[Ca^{2+}]_{in}$ at the same (j_s/j_{dark}). This would result in the observed leftward shift of the GC regulation curve (Fig. 5) without any change of the GC interaction with Ca^{2+}. Similarly, an increase of $[Ca^{2+}]_{in}$ would slow down the phosphorylation of $R*$ by rhodopsin kinase without modifying its regulation via $[Ca^{2+}]_{in}$/recoverin, thus prolonging the PDE activation and increasing the photoresponse.

To test whether the majority of the cAMP-mediated effects could be explained by changed calcium homeostasis, we analyzed photoresponses with a complete model
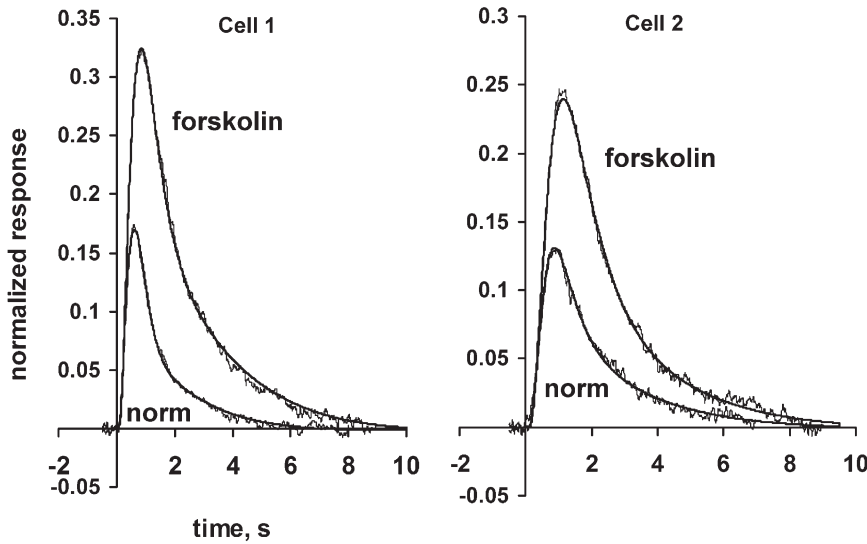
Figure 8. A mathematical model of phototransduction fairly reproduces effects of forskolin on flash photoresponse. "Cell 1" and "Cell 2" refer to the cells' numbers in Tables 1 and S2. Noisy traces, experimental responses; smooth traces, model. For Cell 1, each trace is an average of eight responses (normal solution) or four responses (forskolin solution) to flashes of 0.94 photons $\cdot$ μm^{-2}. For Cell 2, each trace is an average of eight responses (normal solution) or six responses (forskolin solution) to flashes of 0.37 photons $\cdot$ μm^{-2}. For the description of the model, see Materials and methods. Parameters that were modified to imitate forskolin effects are summarized in Table 1. Coefficient of correlation between experimental recordings and model curves, $r^2 > 0.995$.

of rod phototransduction (Kuzmin et al., 2004; Kolesnikov et al., 2011; see Materials and methods). The result of modeling is exemplified in Fig. 8 where we show two cells, one with the fastest and the other with the slowest weak flash responses among those studied. The model revealed that indeed the effect of forskolin can be achieved by a 1.3- to 1.5-fold increase of the fraction of the Ca^{2+} current and a corresponding increase of the dark $[Ca^{2+}]_{in}$. In addition, it was necessary to reduce the dark PDE activity by approximately twofold, decrease maximum GC activity by $\sim$1.2-fold, and slow down quenching of the photoactivated PDE by 1.3–1.4-fold (Table 1). Also, the time constant of arrestin binding to phosphorylated R^* (τ_A) should be adjusted accordingly to Pepperberg's plots for the same cell. All other parameters that characterize PDE activation, Ca^{2+} turnover, and GC and rhodopsin kinase regulation by Ca^{2+} were kept constant.

It should be noted that changes of five of six variable model parameters (increase of Ca^{2+} current and $[Ca^{2+}]_{in}$, inhibition of β_{dark}, decrease of α_{max}, and possible changes of τ_A) are forced and constrained within narrow limits by direct experimental data. Furthermore, four of the five parameters are interrelated and cannot be changed independently. Because the exchanger properties j_{exsat} and K_{Ex} are fixed at their (model) values in normal Ringer's solution, f_{Ca} and Ca_d in forskolin solution must be changed in a concerted way to ensure the correct value of the dark current (for definitions of the parameters see Table S2). Also, β_{dark} and α_{max} are coupled via the necessity to obtain right values of the dark cGMP concentration cG_{dark} and the dark current j_{cGdark}. Therefore, just a single parameter k_E, rate of PDE* turn-off, remained free for fitting. Its decrease is actually the only cAMP-induced change that is inferred from the model rather than directly from the experiment.

Although unexpected, this modeling result is in line with the findings that light adaptation (hence $[Ca^{2+}]_{in}$ decrease) accelerates k_E (Astakhova et al., 2008; Woodruff et al., 2008).

Thus, an increase in intracellular Ca^{2+} appears a parsimonious explanation for most of the forskolin's effects. The mechanism(s) by which cAMP could regulate $[Ca^{2+}]_{in}$ is unclear. Basically unchanged kinetics of the decay of the exchanger current suggests that the activity of the exchanger remains approximately constant. Then, possible targets for cAMP-mediated regulation could be channels that provide the calcium influx into photoreceptor. In the outer segment, the only known channels that might control the calcium influx are CNG channels. The calcium concentration in the outer segment might increase if ionic selectivity of the CNG channels shifted toward a larger fraction of the inward current carried by Ca^{2+}. At present, the only factors that are known to regulate the CNG channels selectivity are membrane voltage and the ionic composition at both

TABLE 1

Model parameters that were varied to simulate the effects of forskolin on flash response (Fig. 8)

Parameter	Cell 1		Cell 2	
	NR	forsk	NR	forsk
I_{cGdark} (pA)	17.8	19	18	18
f_{Ca}	0.15	0.211	0.15	0.19
Ca_d (M)	5×10^{-7}	7×10^{-7}	5×10^{-7}	6.62×10^{-7}
α_{max} (M $\cdot$ s^{-1})	5.87×10^{-6}	4.66×10^{-6}	5.66×10^{-6}	4.91×10^{-6}
β_{dark} (M $\cdot$ s^{-1})	1.659×10^{-6}	0.826×10^{-6}	1.6×10^{-6}	0.833×10^{-6}
k_E (s^{-1})	3.6	2.6	1.81	1.45
τ_A (s)	2	2.6	2.5	2.7

I_{cGdark}, dark current; f_{Ca}, fraction of ROS current carried by Ca^{2+}; Ca_d, dark concentration of free Ca^{2+}; α_{max}, maximum rate of cGMP synthesis achieved at zero Ca^{2+}; β_{dark}, rate of dark cGMP hydrolysis; k_E, rate constant of PDE* turnoff; τ_A, time constant of arrestin binding to phosphorylated rhodopsin.

sides of the plasma membrane (Lagnado et al., 1992; Sheng et al., 2000). It seems unlikely that these parameters are changed by forskolin, as the dark current remains constant.

An alternative target for the cAMP-mediated regulation could be calcium channels in the inner segment. It is shown that forskolin and PKA activator SP-cAMPS decrease Ca^{2+} currents through the L-type voltage-dependent calcium channels in inner segments of salamander rods and small single cones (Stella and Thoreson, 2000). This effect is opposite of what could explain the $[Ca^{2+}]_{in}$ increase suggested by our results.

Cellular location of drug and cAMP targets

The location(s) of targets of drugs used to increase the cAMP concentration in rods, and of targets for cAMP itself, is also uncertain. Little is known about the identity of adenylate cyclase and cAMP-PDE in retinal rods. The presence of adenylate cyclase type 1 was shown in rat photoreceptors (Fukuhara et al., 2004) and cultured chicken photoreceptor (Chaurasia et al., 2006), and the presence of PDE type 8 was demonstrated in the study of mouse photoreceptor proteome (Liu et al., 2007). However, the intracellular localization of neither adenylate cyclase nor cAMP-PDE is known yet. Our attempts to localize the targets by applying the drugs to either the outer or inner segment were inconclusive (Fig. 2 C).

Equally, the cellular localization of targets of cAMP action is also unclear. As mentioned above, the lack of cAMP effect on photoresponse in isolated gecko ROS (Jindrova and Detwiler, 2000) points to the inner segment as the site for cAMP regulation. However, this result allows various explanations, so it is also inconclusive.

Although the explanation of most of the cAMP effects by changed Ca^{2+} homeostasis seems sufficient (whatever is the source of the ion), changes of β_{dark} and α_{max} definitely point to the outer segment as the site for cAMP action as well. Besides, there are other targets in the phototransduction cascade itself, whose properties are modulated by cAMP/PKA. For instance, rod and cone rhodopsin kinases GRK1 and GRK7 in vitro undergo PKA-mediated phosphorylation, which reduces their ability to phosphorylate rhodopsin (Horner et al., 2005). Moreover, the level of phosphorylation of GRK1 and GRK7 is light dependent in vivo, as it is high in the dark-adapted state and low in light (Osawa et al., 2008, 2011). It makes cAMP-dependent GRK phosphorylation a possible candidate for a new pathway of the regulation of rhodopsin turn-off, in addition to the well-known control via recoverin/Ca^{2+}. Also, it is unclear whether the adaptation-dependent control of PDE turn-off (Astakhova et al., 2008; Woodruff et al., 2008) is indeed mediated by Ca^{2+} rather than by other mechanisms, possibly involving cAMP.

Regardless of specific molecular mechanisms to be elucidated, our data show that all effects of the elevated cAMP in the phototransduction cascade work synergistically, increasing photoreceptor sensitivity. Increase of the cAMP level while photoreceptor cells adjust from day to night light conditions and increase of their sensitivity are likely to have adaptive significance and improve the visual system performance in twilight conditions.

REFERENCES

Arshavsky, V.Y., and M.E. Burns. 2012. Photoreceptor signaling: supporting vision across a wide range of light intensities. *J. Biol. Chem.* 287:1620–1626. http://dx.doi.org/10.1074/jbc.R111.305243

Astakhova, L.A., M.L. Firsov, and V.I. Govardovskii. 2008. Kinetics of turn-offs of frog rod phototransduction cascade. *J. Gen. Physiol.* 132:587–604. http://dx.doi.org/10.1085/jgp.200810034

Baylor, D.A., T.D. Lamb, and K.W. Yau. 1979. The membrane current of single rod outer segments. *J. Physiol.* 288:589–611.

Besharse, J.C., D.A. Dunis, and B. Burnside. 1982. Effects of cyclic adenosine 3′,5′-monophosphate on photoreceptor disc shedding and retinomotor movement. Inhibition of rod shedding and stimulation of cone elongation. *J. Gen. Physiol.* 79:775–790. http://dx.doi.org/10.1085/jgp.79.5.775

Bitensky, M.W., R.E. Gorman, and W.H. Miller. 1971. Adenyl cyclase as a link between photon capture and changes in membrane permeability of frog photoreceptors. *Proc. Natl. Acad. Sci. USA.* 68:561–562. http://dx.doi.org/10.1073/pnas.68.3.561

Burns, M.E., and D.A. Baylor. 2001. Activation, deactivation, and adaptation in vertebrate photoreceptor cells. *Annu. Rev. Neurosci.* 24:779–805. http://dx.doi.org/10.1146/annurev.neuro.24.1.779

Burnside, B., M. Evans, R.T. Fletcher, and G.J. Chader. 1982. Induction of dark-adaptive retinomotor movement (cell elongation) in teleost retinal cones by cyclic adenosine 3′,′5-monophosphate. *J. Gen. Physiol.* 79:759–774. http://dx.doi.org/10.1085/jgp.79.5.759

Chaurasia, S.S., R. Haque, N. Pozdeyev, C.R. Jackson, and P.M. Iuvone. 2006. Temporal coupling of cyclic AMP and Ca/calmodulin-stimulated adenylyl cyclase to the circadian clock in chick retinal photoreceptor cells. *J. Neurochem.* 99:1142–1150. http://dx.doi.org/10.1111/j.1471-4159.2006.04154.x

Demontis, G.C., G.M. Ratto, S. Bisti, and L. Cervetto. 1995. Effect of blocking the Na^+/K^+ ATPase on Ca^{2+} extrusion and light adaptation in mammalian retinal rods. *Biophys. J.* 69:439–450. http://dx.doi.org/10.1016/S0006-3495(95)79917-9

Fesenko, E.E., S.S. Kolesnikov, and A.L. Lyubarsky. 1985. Induction by cyclic GMP of cationic conductance in plasma membrane of retinal rod outer segment. *Nature.* 313:310–313. http://dx.doi.org/10.1038/313310a0

Fukuhara, C., C. Liu, T.N. Ivanova, G.C. Chan, D.R. Storm, P.M. Iuvone, and G. Tosini. 2004. Gating of the cAMP signaling cascade and melatonin synthesis by the circadian clock in mammalian retina. *J. Neurosci.* 24:1803–1811. http://dx.doi.org/10.1523/JNEUROSCI.4988-03.2004

Govardovskii, V.I., and A.L. Berman. 1981. Light-induced changes of cyclic GMP content in frog retinal rod outer segments measured

with rapid freezing and microdissection. *Biophys. Struct. Mech.* 7:125–130. http://dx.doi.org/10.1007/BF00539174

Hasegawa, M., and G.M. Cahill. 1999. A role for cyclic AMP in entrainment of the circadian oscillator in Xenopus retinal photoreceptors by dopamine but not by light. *J. Neurochem.* 72:1812–1820. http://dx.doi.org/10.1046/j.1471-4159.1999.0721812.x

Hodgkin, A.L., and B.J. Nunn. 1988. Control of light-sensitive current in salamander rods. *J. Physiol.* 403:439–471.

Hodgkin, A.L., P.A. McNaughton, and B.J. Nunn. 1985. The ionic selectivity and calcium dependence of the light-sensitive pathway in toad rods. *J. Physiol.* 358:447–468.

Horner, T.J., S. Osawa, M.D. Schaller, and E.R. Weiss. 2005. Phosphorylation of GRK1 and GRK7 by cAMP-dependent protein kinase attenuates their enzymatic activities. *J. Biol. Chem.* 280:28241–28250. http://dx.doi.org/10.1074/jbc.M505117200

Iuvone, P.M., and J.C. Besharse. 1986. Cyclic AMP stimulates serotonin N-acetyltransferase activity in *Xenopus* retina in vitro. *J. Neurochem.* 46:33–39. http://dx.doi.org/10.1111/j.1471-4159.1986.tb12921.x

Ivanova, T.N., and P.M. Iuvone. 2003. Circadian rhythm and photic control of cAMP level in chick retinal cell cultures: a mechanism for coupling the circadian oscillator to the melatonin-synthesizing enzyme, arylalkylamine N-acetyltransferase, in photoreceptor cells. *Brain Res.* 991:96–103. http://dx.doi.org/10.1016/j.brainres.2003.08.003

Ivanova, T.N., A.L. Alonso-Gomez, and P.M. Iuvone. 2008. Dopamine D4 receptors regulate intracellular calcium concentration in cultured chicken cone photoreceptor cells: relationship to dopamine receptor-mediated inhibition of cAMP formation. *Brain Res.* 1207:111–119. http://dx.doi.org/10.1016/j.brainres.2008.02.025

Jackson, C.R., S.S. Chaurasia, H. Zhou, R. Haque, D.R. Storm, and P.M. Iuvone. 2009. Essential roles of dopamine D4 receptors and the type 1 adenylyl cyclase in photic control of cyclic AMP in photoreceptor cells. *J. Neurochem.* 109:148–157. http://dx.doi.org/10.1111/j.1471-4159.2009.05920.x

Janisch, K.M., J.M. Kasanuki, M.C. Naumann, R.J. Davis, C.S. Lin, S. Semple-Rowland, and S.H. Tsang. 2009. Light-dependent phosphorylation of the gamma subunit of cGMP-phophodiesterase (PDE6gamma) at residue threonine 22 in intact photoreceptor neurons. *Biochem. Biophys. Res. Commun.* 390:1149–1153. http://dx.doi.org/10.1016/j.bbrc.2009.10.106

Jindrova, H., and P.B. Detwiler. 2000. Cyclic AMP has no effect on the generation, recovery, or background adaptation of light responses in functionally intact rod outer segments: with implications about the function of phosducin. *Vis. Neurosci.* 17:887–892. http://dx.doi.org/10.1017/S0952523800176072

Ko, G.Y., M.L. Ko, and S.E. Dryer. 2004. Circadian regulation of cGMP-gated channels of vertebrate cone photoreceptors: role of cAMP and Ras. *J. Neurosci.* 24:1296–1304. http://dx.doi.org/10.1523/JNEUROSCI.3560-03.2004

Koch, K.W., and L. Stryer. 1988. Highly cooperative feedback control of retinal rod guanylate cyclase by calcium ions. *Nature.* 334:64–66. http://dx.doi.org/10.1038/334064a0

Kolesnikov, A.V., L. Rikimaru, A.K. Hennig, P.D. Lukasiewicz, S.J. Fliesler, V.I. Govardovskii, V.J. Kefalov, and O.G. Kisselev. 2011. G-protein betagamma-complex is crucial for efficient signal amplification in vision. *J. Neurosci.* 31:8067–8077. http://dx.doi.org/10.1523/JNEUROSCI.0174-11.2011

Kuzmin, D.G., M.L. Firsov, and V.I. Govardovskii. 2004. Mathematical modeling of phototransduction and light adaptation in frog retinal rods. *Sens. Syst.* 18:305–316.

Lagnado, L., L. Cervetto, and P.A. McNaughton. 1992. Calcium homeostasis in the outer segments of retinal rods from the tiger salamander. *J. Physiol.* 455:111–142.

Lamb, T.D., and E.N. Pugh Jr. 2006. Phototransduction, dark adaptation, and rhodopsin regeneration. The Proctor lecture. *Invest. Ophthalmol. Vis. Sci.* 47:5137–5152. http://dx.doi.org/10.1167/iovs.06-0849

Li, P., S.S. Chaurasia, Y. Gao, A.L. Carr, P.M. Iuvone, and L. Li. 2008. CLOCK is required for maintaining the circadian rhythms of Opsin mRNA expression in photoreceptor cells. *J. Biol. Chem.* 283:31673–31678. http://dx.doi.org/10.1074/jbc.M803875200

Lipton, S.A., H. Rasmussen, and J.E. Dowling. 1977. Electrical and adaptive properties of rod photoreceptors in *Bufo marinus.* II. Effects of cyclic nucleotides and prostaglandins. *J. Gen. Physiol.* 70:771–791. http://dx.doi.org/10.1085/jgp.70.6.771

Liu, Q., G. Tan, N. Levenkova, T. Li, E.N. Pugh Jr., J.J. Rux, D.W. Speicher, and E.A. Pierce. 2007. The proteome of the mouse photoreceptor sensory cilium complex. *Mol. Cell. Proteomics.* 6:1299–1317. http://dx.doi.org/10.1074/mcp.M700054-MCP200

Miki, N., J.J. Keirns, F.R. Marcus, J. Freeman, and M.W. Bitensky. 1973. Regulation of cyclic nucleotide concentrations in photoreceptors: an ATP-dependent stimulation of cyclic nucleotide phosphodiesterase by light. *Proc. Natl. Acad. Sci. USA.* 70:3820–3824. http://dx.doi.org/10.1073/pnas.70.12.3820

Nakatani, K., and K.W. Yau. 1989. Sodium-dependent calcium extrusion and sensitivity regulation in retinal cones of the salamander. *J. Physiol.* 409:525–548.

Nir, I., J.M. Harrison, R. Haque, M.J. Low, D.K. Grandy, M. Rubinstein, and P.M. Iuvone. 2002. Dysfunctional light-evoked regulation of cAMP in photoreceptors and abnormal retinal adaptation in mice lacking dopamine D4 receptors. *J. Neurosci.* 22:2063–2073.

Osawa, S., R. Jo, and E.R. Weiss. 2008. Phosphorylation of GRK7 by PKA in cone photoreceptor cells is regulated by light. *J. Neurochem.* 107:1314–1324. http://dx.doi.org/10.1111/j.1471-4159.2008.05691.x

Osawa, S., R. Jo, Y. Xiong, B. Reidel, N. Tserentsoodol, V.Y. Arshavsky, P.M. Iuvone, and E.R. Weiss. 2011. Phosphorylation of G protein-coupled receptor kinase 1 (GRK1) is regulated by light but independent of phototransduction in rod photoreceptors. *J. Biol. Chem.* 286:20923–20929. http://dx.doi.org/10.1074/jbc.M111.230904

Pagh-Roehl, K., D. Lin, L. Su, and B. Burnside. 1995. Phosducin and PP33 are in vivo targets of PKA and type 1 or 2A phosphatases, regulators of cell elongation in teleost rod inner-outer segments. *J. Neurosci.* 15:6475–6488.

Paglia, M.J., H. Mou, and R.H. Cote. 2002. Regulation of photoreceptor phosphodiesterase (PDE6) by phosphorylation of its inhibitory gamma subunit re-evaluated. *J. Biol. Chem.* 277:5017–5023. http://dx.doi.org/10.1074/jbc.M106328200

Pepperberg, D.R., M.C. Cornwall, M. Kahlert, K.P. Hofmann, J. Jin, G.J. Jones, and H. Ripps. 1992. Light-dependent delay in the falling phase of the retinal rod photoresponse. *Vis. Neurosci.* 8:9–18. http://dx.doi.org/10.1017/S0952523800006441

Peshenko, I.V., E.V. Olshevskaya, and A.M. Dizhoor. 2004. Ca^{2+}-dependent conformational changes in guanylyl cyclase-activating protein 2 (GCAP-2) revealed by site-specific phosphorylation and partial proteolysis. *J. Biol. Chem.* 279:50342–50349. http://dx.doi.org/10.1074/jbc.M408683200

Peshenko, I.V., E.V. Olshevskaya, A.B. Savchenko, S. Karan, K. Palczewski, W. Baehr, and A.M. Dizhoor. 2011. Enzymatic properties and regulation of the native isozymes of retinal membrane guanylyl cyclase (RetGC) from mouse photoreceptors. *Biochemistry.* 50:5590–5600. http://dx.doi.org/10.1021/bi200491b

Pierce, M.E., D. Barker, J. Harrington, and J.S. Takahashi. 1989. Cyclic AMP-dependent melatonin production in Y79 human retinoblastoma cells. *J. Neurochem.* 53:307–310. http://dx.doi.org/10.1111/j.1471-4159.1989.tb07330.x

Pugh, E.N., Jr., and T.D. Lamb. 2000. Phototransduction in vertebrate rods and cones: molecular mechanisms of amplification, recovery and light adaptation. *In* Handbook of Biological Physics. D.G. Stavenga, E.N. Pugh Jr., and W.J. de Grip, editors. Elsevier Science, Amsterdam. 183–255.

Sheng, J.Z., C.F. Prinsen, R.B. Clark, W.R. Giles, and P.P. Schnetkamp. 2000. Na^+-Ca^{2+}-K^+ currents measured in insect cells transfected with the retinal cone or rod Na^+-Ca^{2+}-K^+ exchanger cDNA. *Biophys. J.* 79:1945–1953. http://dx.doi.org/10.1016/S0006-3495(00)76443-5

Sokolov, M., A.L. Lyubarsky, K.J. Strissel, A.B. Savchenko, V.I. Govardovskii, E.N. Pugh Jr., and V.Y. Arshavsky. 2002. Massive light-driven translocation of transducin between the two major compartments of rod cells: a novel mechanism of light adaptation. *Neuron.* 34:95–106.

Stella, S.L., Jr., and W.B. Thoreson. 2000. Differential modulation of rod and cone calcium currents in tiger salamander retina by D2 dopamine receptors and cAMP. *Eur. J. Neurosci.* 12:3537–3548. http://dx.doi.org/10.1046/j.1460-9568.2000.00235.x

Tosini, G., N. Pozdeyev, K. Sakamoto, and P.M. Iuvone. 2008. The circadian clock system in the mammalian retina. *Bioessays.* 30:624–633. http://dx.doi.org/10.1002/bies.20777

Traverso, V., R.A. Bush, P.A. Sieving, and D. Deretic. 2002. Retinal cAMP levels during the progression of retinal degeneration in rhodopsin P23H and S334ter transgenic rats. *Invest. Ophthalmol. Vis. Sci.* 43:1655–1661.

Tsang, S.H., M.L. Woodruff, K.M. Janisch, M.C. Cilluffo, D.B. Farber, and G.L. Fain. 2007. Removal of phosphorylation sites of gamma subunit of phosphodiesterase 6 alters rod light response. *J. Physiol.* 579:303–312. http://dx.doi.org/10.1113/jphysiol.2006.121772

Willardson, B.M., J.F. Wilkins, T. Yoshida, and M.W. Bitensky. 1996. Regulation of phosducin phosphorylation in retinal rods by Ca^{2+}/calmodulin-dependent adenylyl cyclase. *Proc. Natl. Acad. Sci. USA.* 93:1475–1479. http://dx.doi.org/10.1073/pnas.93.4.1475

Wolbring, G., and P.P. Schnetkamp. 1996. Modulation of the calcium sensitivity of bovine retinal rod outer segment guanylyl cyclase by sodium ions and protein kinase A. *Biochemistry.* 35:11013–11018. http://dx.doi.org/10.1021/bi960699e

Woodruff, M.L., K.M. Janisch, I.V. Peshenko, A.M. Dizhoor, S.H. Tsang, and G.L. Fain. 2008. Modulation of phosphodiesterase6 turnoff during background illumination in mouse rod photoreceptors. *J. Neurosci.* 28:2064–2074. http://dx.doi.org/10.1523/JNEUROSCI.2973-07.2008

Xu, L.X., Y. Tanaka, V.A. Bonderenko, I. Matsuura, H. Matsumoto, A. Yamazaki, and F. Hayashi. 1998. Phosphorylation of the gamma subunit of the retinal photoreceptor cGMP phosphodiesterase by the cAMP-dependent protein kinase and its effect on the gamma subunit interaction with other proteins. *Biochemistry.* 37:6205–6213. http://dx.doi.org/10.1021/bi973087i

Yau, K.W., and R.C. Hardie. 2009. Phototransduction motifs and variations. *Cell.* 139:246–264. http://dx.doi.org/10.1016/j.cell.2009.09.029